Journal of Power Sources 196 (2011) 10240–10243

Contents lists available at ScienceDirect

Journal of Power Sources

journal homepage: www.elsevier.com/locate/jpowsour

Short communication

Carbon-coated SiO_2 nanoparticles as anode material for lithium ion batteries

Yu Yao, Jingjing Zhang, Leigang Xue, Tao Huang, Aishui Yu*

Department of Chemistry, Shanghai Key Laboratory of Molecular Catalysis and Innovative Materials, Institute of New Energy, Fudan University, Shanghai 200438, China

ARTICLE INFO

Article history:
Received 28 April 2011
Received in revised form 24 June 2011
Accepted 2 August 2011
Available online 9 August 2011

Keywords:
Silica
Lithium ion batteries
Anode material
Carbon coating

ABSTRACT

A simple approach is proposed to prepare C-SiO_2 composites as anode materials for lithium ion batteries. In this novel approach, nano-sized silica is soaked in sucrose solution and then heat treated at 900 °C under nitrogen atmosphere. Transmission electron microscopy (TEM) and X-ray diffraction (XRD) analysis shows that SiO_2 is embedded in amorphous carbon matrix. The electrochemical test results indicate that the electrochemical performance of the C-SiO_2 composites relates to the SiO_2 content of the composite. The C-SiO_2 composite with 50.1% SiO_2 shows the best reversible lithium storage performance. It delivers an initial discharge capacity of 536 mAh g^{-1} and good cyclability with the capacity of above 500 mAh g^{-1} at 50th cycle. Electrochemical impedance spectra (EIS) indicates that the carbon layer coated on SiO_2 particles can diminish interfacial impedance, which leads to its good electrochemical performance.

1. Introduction

Lithium-ion battery (LIB) with high energy density is in great demand as an energy source for many applications. Carbon anode material has the advantages of long cycle life and low cost, however, its low Lithium-storage capacity cannot satisfy future requirements of the electronic devices and electric vehicles. Silicon and some metals (e.g. Sn, Si, Sb) which could alloy with lithium have higher theoretical specific capacity. These materials were exploited as anode materials to replace the current carbon-based materials [1–8], but they have disadvantages of poor mechanical and cycling stability caused by drastic volume changes in charge and discharge processes. To solve this problem, metallic oxides and metallic oxide-based glasses have been proposed as alternative anode materials. Lithium insertion into metal oxides produces an inert Li_2O matrix, which could support and disperse active metal domains. The matrix can greatly decrease the volume change effect and improve the cyclability [9–15]. It was reported that silicon monoxide (SiO) has a reversible capacity greatly higher than carbon materials [16–18]. The Si–C–O material was also prepared and showed high reversible capacity [19,20]. Gao et al. claimed that commercial SiO_2 nanoparticles (7 nm in diameter) can react with Li between 0.0 and 1.0 V (vs. Li/Li^+) with a reversible capacity of 400 mAh g^{-1} [21]. Guo et al. prepared a HC-SiO_2 composite and their tests proved the electrochemical reduction of nano-SiO_2 and the formation of Li_4SiO_4 and Li_2O as well as Si in the first-discharge process [22].

In this work, carbon-coated SiO_2 was prepared by simply soaking the nano-SiO_2 in sucrose solution, followed by drying and carbonization in an inert atmosphere. The pyrolysis product of sucrose coating on SiO_2 particle formed a hard-carbon layer and then the C-SiO_2 composites were investigated as anode materials for lithium ion battery.

2. Experimental

2.1. Preparation of C-SiO_2 composites

Sucrose was dissolved in deionized water with continuous stirring. Subsequently, different quantities of SiO_2 nanoparticles (7 nm in diameter, AEROSIL) were added into the sucrose solution. The weight ratio of SiO_2 to sucrose was ranging from 5:8 to 1:8. The mixture was then steadily agitated to ensure that SiO_2 disperses throughout the solution and evaporating water at 60 °C to give a solid blend. The mixture was heated at 900 °C in a nitrogen atmosphere for 3 h and cooled down to room temperature naturally. The carbon-coated SiO_2 nanoparticles with various carbon contents were obtained.

2.2. Characterization

The content of carbon in the composite was determined from the ignition loss of the sample at 800 °C in air with a thermo gravimetric and differential thermal (TGA/DTA) apparatus (DTG-60H, Shimadz). Fourier-transform infrared reflection (FTIR) spectra were recorded on a Shimadz IRPrestige-21 FTIR spectrometer using KBr pellet. The morphology of as-prepared carbon-coated SiO_2 was observed by scanning electron microscopy (SEM, FE-SEMS-4800,

* Corresponding author. Tel.: +86 21 51630320; fax: +86 21 51630320.
E-mail address: asyu@fudan.edu.cn (A. Yu).

0378-7753/$ – see front matter © 2011 Elsevier B.V. All rights reserved.
doi:10.1016/j.jpowsour.2011.08.009

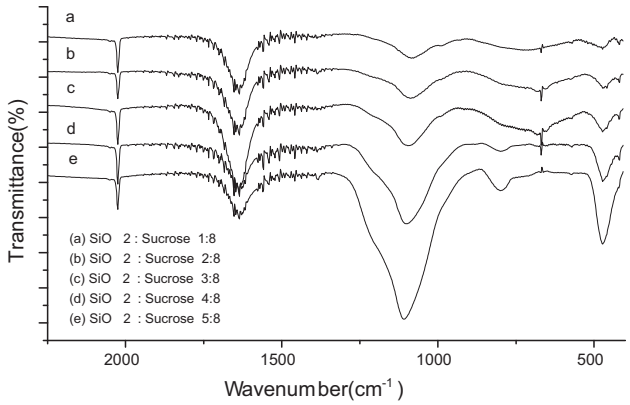

Fig. 1. Fourier transform infrared spectroscopy of carbon coated SiO_2 particles with different carbon contents.

Hitachi) and transmission electron microscopy (TEM, JEM-2100F, Japan). X-ray diffraction (XRD) pattern was performed on a Brüker D8 Advance and Davinci Design X-ray diffractometer using Cu Kα radiation with a λ of 1.5406 Å at a scan rate of 4° min^{-1} from 10° to 90°.

2.3. Electrochemical measurement

The electrochemical performance of the as-prepared carbon-coated SiO_2 materials was evaluated using coin cells assembled in an argon-filled glove box (Mikarouna, Superstar 1220/750/900). An assembled coin cell was composed of lithium as the counter electrode and the working electrode prepared by active materials, super P carbon black and polyvinylidene fluoride (PVDF) with a weight ratio of 80:10:10, using 1-methyl-2-pyrrolidinone (NMP) as the solvent onto a copper foil. The resulting film was dried at 80 °C in vacuum for 12 h in order to evaporate the NMP. 1 M $LiPF_6$ was dissolved in a mixed solvent of ethylene carbonate (EC) and dimethyl carbonate (DMC) (1:1 in weight) to act as the electrolyte and microporous polypropylene film (Celgard 2300) was used as separator. The total mass of active electrode material is about 4 mg and electrode surface area is 1.54 cm^2 (ϕ 14 mm). The electrochemical performance of the as-prepared materials was tested by cyclic voltammetry, galvanostatically charging and discharging tests and electrochemical impedance spectroscopy (EIS). Cyclic voltammetry was carried out in the potential range from open-circuit potential (OCP) to 0 V (vs. Li/Li^+), at a scan rate of 0.1 mV s^{-1} on an electrochemical workstation (CH Instrument 660A, CHI Company). The galvanostatic charge–discharge tests were performed on a battery test system (Land CT2001A, Wuhan Jinnuo Electronic Co. Ltd.) at a constant current density of 50 mA g^{-1} in the potential range from 0 to 3.0 V. EIS measurements were measured for the fresh cells at open potential with an ac amplitude of 5 mV over the frequency range from 100k to 0.01 Hz.

3. Results and discussion

Fig. 1 is the FTIR spectra of carbon-coated SiO_2 nanoparticles with different carbon contents. There are three characteristic peaks attributed to SiO_2. The peaks at 1102, 798, 472 cm^{-1} can be assigned to asymmetry Si–O–Si bond stretching, SiO_4 tetrahedron ring, and O–Si–O bond deformation, respectively. With the reduction of initial ratio of SiO_2, the intensity of the three peaks decreased.

Thermal gravimetric results (shown in Table 1) give the actual content of SiO_2 in the C-SiO_2 composites. Compared with carbon-coated SiO_2 nanoparticles, same proportion of carbon black (super P) which is similar to hard carbon pyrolysis from sucrose was mixed with SiO_2 nanoparticles by milling. Electrochemical test of both materials have been done and their first discharge capacity data are shown in Table 1. It can be seen that first discharge capacity of carbon-coated SiO_2 nanoparticles increased slightly with the increase of carbon. But when the content of SiO_2 is lower than 50%, the capacity begins to decrease. The sample with 50.1% SiO_2 exhibits the highest specific capacity. For super P carbon black mixed SiO_2 nanoparticles, the first discharge capacity increases with the decreasing of SiO_2 content, but is lower than the corresponding carbon-coated ones.

Table 1
Electrochemical performance of the carbon coated SiO_2 and super P carbon black mixed SiO_2.

SiO_2:sucrose	Actual SiO_2 content (wt.%)	First discharge capacity of carbon coated SiO_2 (mAh g^{-1})	First discharge capacity of carbon mixed with same proportion SiO_2 (mAh g^{-1})
5:8	81.0	480.1	67.7
4:8	69.5	476.8	107.0
3:8	64.1	519.9	112.6
2:8	50.1	535.9	137.2
1:8	35.8	357.3	176.9

Fig. 2a displays SEM images of the pure SiO_2 nanoparticles. The diameter of single particle is about 10 nm. Fig. 2b shows the carbon-coated SiO_2 nanoparticles with the content of SiO_2 content of 50.1%.

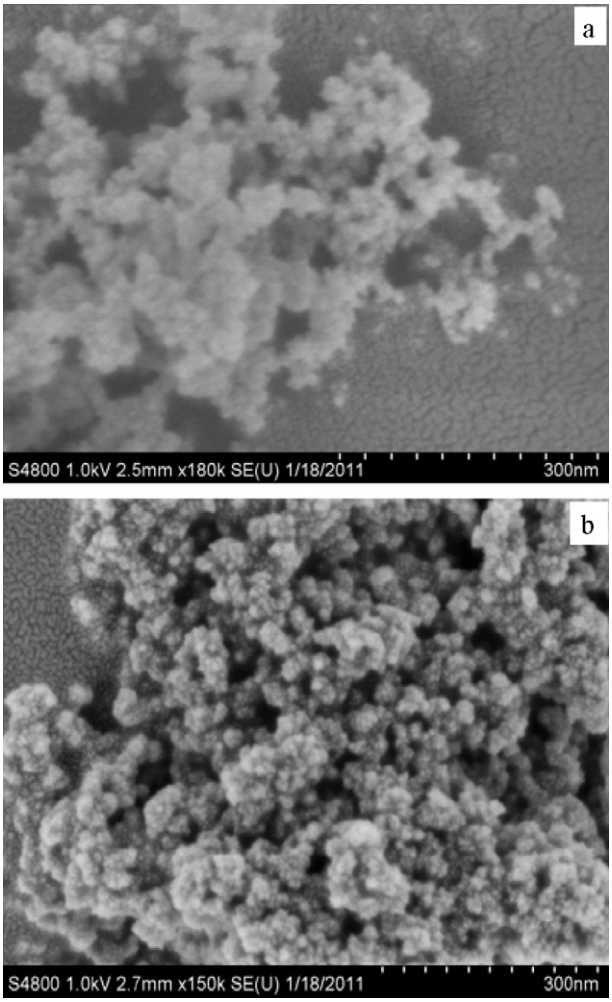

Fig. 2. SEM images of SiO_2 nanoparticles (a) and carbon coated SiO_2 nanoparticles with 50.1% SiO_2 (b).

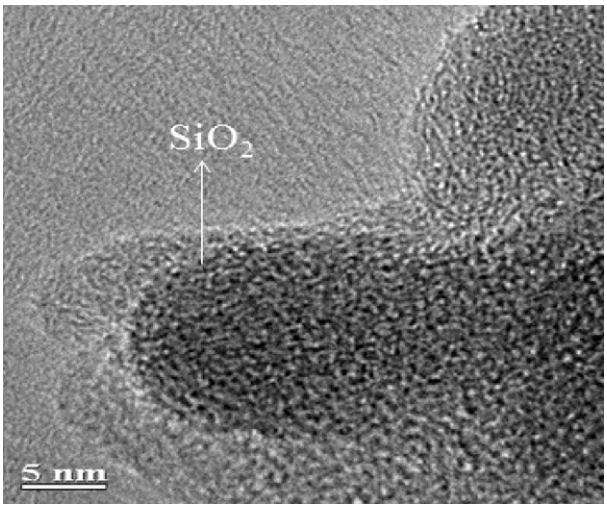

Fig. 3. TEM image of carbon coated SiO_2 nanoparticles with 50.1% SiO_2.

It can be seen that the diameter of SiO_2 particles increases to 20 nm which could be due to the carbon coating layer.

Fig. 3 shows TEM images of the carbon-coated SiO_2 nanoparticles with 50.1% SiO_2. It can be clearly seen that the SiO_2 particles are coated with carbon. The dark area in centre is the SiO_2 particle, with diameter of about 10 nm, which is consistent with the result of SEM image.

Fig. 4a shows XRD pattern of pure SiO_2 nanoparticles. The broad band indicates that the structure of SiO_2 nanoparticles is amorphous. Fig. 3b gives XRD pattern of carbon-coated SiO_2 nanoparticles with 50.1% SiO_2. The wide peaks at about 22° (0 0 2), 43° (1 0 0) are attributed to the carbon layer coated on SiO_2 nanoparticles and the structure of carbon layer is also amorphous. There is no peak of silicon could be found, which manifests SiO_2 was not reduced to Si. It was reported that SiO_2 cannot be reduced to glass-like compounds such as $SiO_{2-\delta}$ or Si–C–O by carbon at 1000 °C [22].

Impedance experiments were applied to explore the effect of carbon layer coated on SiO_2 nanoparticles on the interfacial impedance of C-SiO_2 composite. Fig. 5 shows Nyquist plots of the carbon-coated SiO_2 particles and the carbon black mixed SiO_2 particles before cycling. The semicircle shows that interfacial impedance become smaller with the reduction of SiO_2 content, which means SiO_2 particles are coated more uniformly by carbon [23]. The interfacial impedance of carbon coated SiO_2 (Fig. 5a) is lower than the corresponding carbon mixed one (Fig. 5b). It means the carbon coated samples have better effects in reducing interfacial impedance than the carbon mixed samples. The EIS plots account for the increase of the first discharge capacity with the raise of carbon content, which is shown in Table 1. However, the further reduction of active material SiO_2 led to discharge capacity fade, resulting in the decrease of discharge capacity when the SiO_2 content is below 50%.

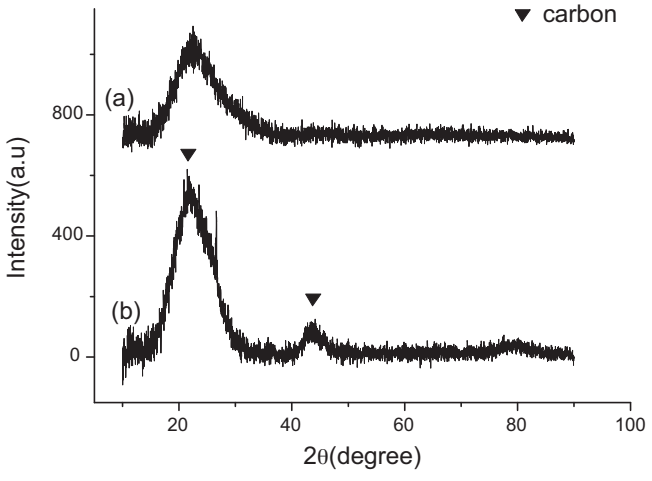

Fig. 4. XRD patterns of SiO_2 nanoparticles (a) and carbon coated SiO_2 nanoparticles with 50.1% SiO_2 (b).

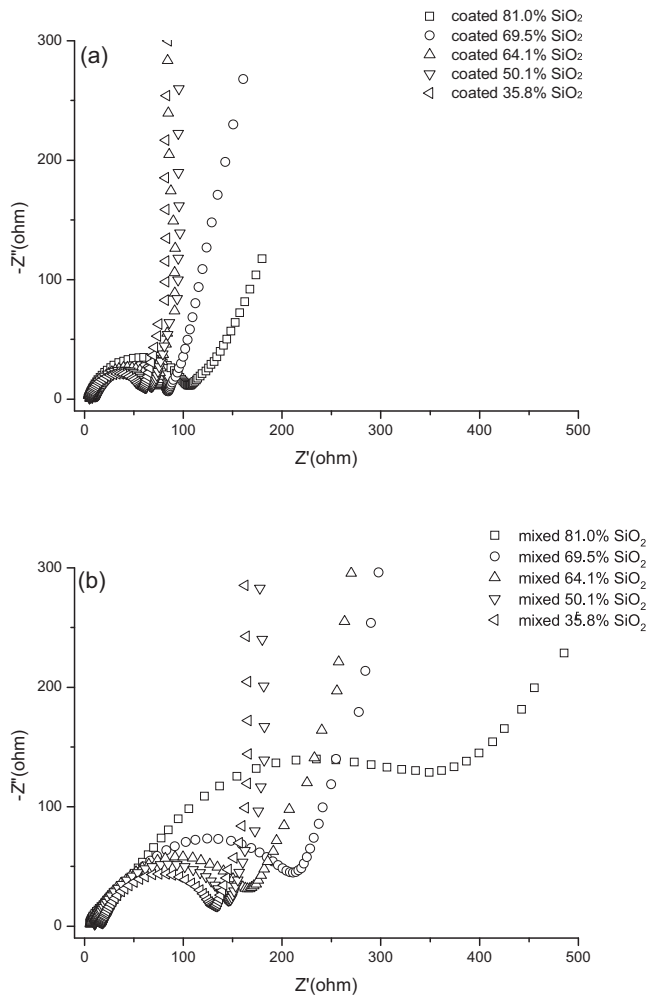

Fig. 5. Electrochemical impedance spectra of carbon coated SiO_2 nanoparticles (a) and super P black mixed SiO_2 nanoparticles (b).

The charge–discharge profiles of carbon coated SiO_2 nanoparticles with 50.1% SiO_2 is shown in Fig. 6a. The first discharge capacity of the composite is 536 mAh g^{-1}, which is much higher than carbonaceous materials. The charging profile is very steep at potentials exceeding 1.5 V, but not flat as graphite. It owning to the large polarization of the glassy material derived from the SiO_2. The Si generated during the first conversion cycle has poor conductivity and hinders the kinetics of Li alloying, though the active material particle size distribution is around 20 nm. There are two plateaus at 0.69 V and 0.15 V in first discharge curve (Fig. 6a), corresponding to the two peaks in cyclic voltammogram (Fig. 6b). The peak at 0.69 V is associated with the electrolyte decomposition and the formation of the solid electrolyte interface (SEI) layer, which contributes about 100 mAh g^{-1} to the total irreversible capacity of the cell (ca. 355 mAh g^{-1}). The other peak at 0.15 V is related to electrochemical reactions between lithium ions and SiO_2 in the composite and contributing the other irreversible capacity. This electrochemi-

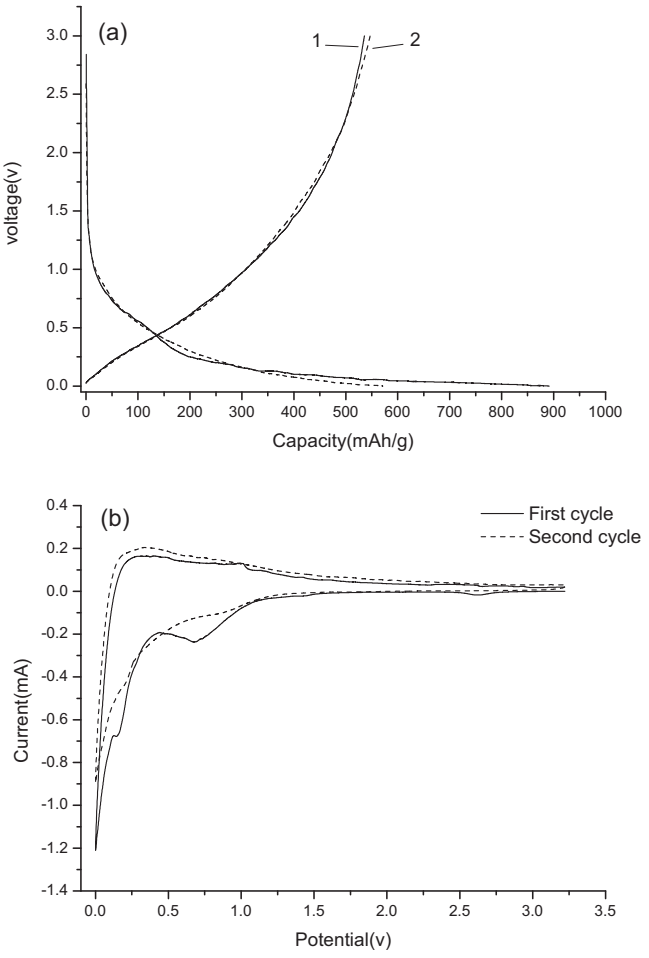

Fig. 6. The charge–discharge profiles (a) and cyclic voltammogram (b) of carbon coated SiO_2 nanoparticles with 50.1% SiO_2 of first two cycles.

cal reaction involves amorphous nano-SiO_2 being reduced to Si and forming amorphous Li_2O or crystalline Li_4SiO_4 [22]. These reactions can be summarized as follows:

$$SiO_2 + 4Li^+ + 4e^- \rightarrow 2Li_2O + Si \quad (1a)$$

$$2SiO_2 + 4Li^+ + 4e^- \rightarrow Li_4SiO_4 + Si \quad (1b)$$

$$Si + xLi^+ + xe^- \leftrightarrow Li_xSi \quad (2)$$

As both reaction (1a) and (1b) were irreversible, the formation of SEI layer and SiO_2 reduction accounted for irreversible capacity.

Fig. 7 shows cycling performance of carbon-coated SiO_2 particles with different carbon contents. It is found that the cycle life improved with the increase of carbon content, because the carbon matrix can provide a stable structure to buffer the drastic volume changes during discharge and charge process. The composite with 50.1% SiO_2 shows the best storage capacity, which remains above 500 mAh g^{-1} at 50th cycle. The reasons for the good cyclability of the composite could be attributed to that nano-sized of particle greatly decreases the volume changes in lithium ion insertion and extraction, and meanwhile, Li_2O or Li_4SiO_4 formed in the first discharge process results in an inert matrix which can support and disperse active Si domains, and accommodate volume changes during the alloying and dealloying reactions with lithium ions. The coated carbon layer might also act as the constrained force for volume change during cycling.

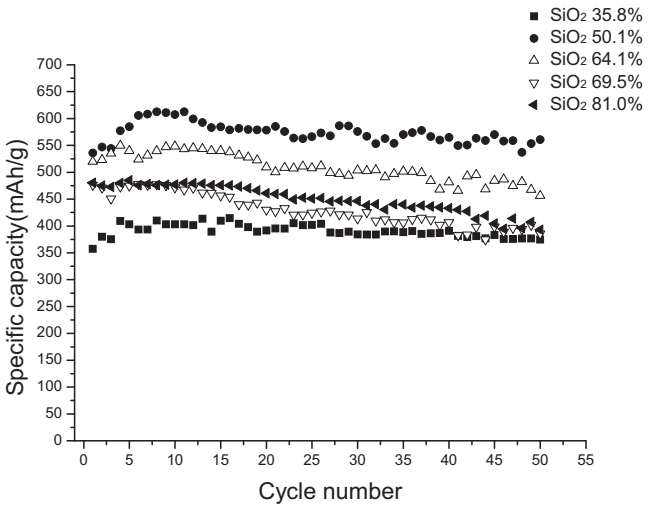

Fig. 7. Cycling performance of carbon coated SiO_2 particles with different carbon contents.

4. Conclusions

Carbon-coated SiO_2 nanoparticles prepared by nesting nano-sized SiO_2 particles in carbon cage. It showed high storage capacity and good cyclability. The results indicate that coated carbon could lead to lower interfacial impedance and higher storage capacity. The composite with 50.1% SiO_2 gives the largest storage capacity, which remains above 500 mAh g^{-1} at 50th cycle. The good cyclability of the C-SiO_2 composite attributes to that nano-sized of particle and Li_2O or Li_4SiO_4 formed during first discharge process alleviates the volume change in lithium ion insertion and extraction. Besides, the coated carbon layer restrain electrode pulverized during charge and discharge processes.

References

[1] J.L. Tirado, Mater. Sci. Eng. R40 (2003) 103–136.
[2] T. Morishita, T. Hirabayashi, T. Okuni, N. Ota, M. Inagaki, J. Power Sources 160 (2006) 638–644.
[3] B.K. Guo, J. Shu, K. Tang, Y. Bai, Z.X. Wang, L.Q. Chen, J. Power Sources 177 (2008) 205–210.
[4] Z.S. Wen, J. Yang, B.F. Wang, K. Wang, Y. Liu, Electrochem. Commun. 5 (2003) 165–168.
[5] N. Dimov, S. Kugino, M. Yoshio, Electrochim. Acta 48 (2003) 1579–1587.
[6] T. Hasegawa, S.R. Mukai, Y. Shirato, H. Tamon, Carbon 42 (2004) 2573–2579.
[7] V.G. Khomenko, V.Z. Barsukov, Electrochim. Acta 52 (2007) 2829–2840.
[8] Z. Lao, D.D. Fan, X.L. Lin, H.Y. Mao, C.F. Yao, Z.Y. Deng, J. Power Sources 189 (2009) 16–21.
[9] Y. Idota, T. Kubota, A. Matsufuji, Y. Maekawa, T. Miyasaka, Science 276 (1997) 1395.
[10] I.A. Courtney, J.R. Dahn, J. Electrochem. Soc. 144 (1997) 2045.
[11] H. Morimoto, M. Tatsumisago, T. Minami, Electrochem. Solid State Lett. 4 (2001) A16.
[12] J. Read, D. Foster, J. wolfenstine, W. Behl, J. Power Sources 96 (2001) 277–281.
[13] L. Yuan, K. Konstantinov, G.X. Wang, H.K. Liu, S.X. Dou, J. Power Sources 146 (2005) 180–184.
[14] G.X. Wang, Y. Chen, K. Konstantinov, J. Yao, J. Ahn, H.K. Liu, S.X. Dou, J. Alloys Compd. 340 (2002) L5–L10.
[15] Y. Lu, Y. Wang, Y. Zou, Z. Jiao, B. Zhao, Y.Q. He, M.H. Wu, Electrochem. Commun. 12 (2010) 101–105.
[16] J. Yang, Y. Takeda, N. Imanishi, C. Capiglia, J.Y. Xie, O. Yamamoto, Solid State Ionics 125 (2002) 152–153.
[17] T. Kim, S. Park, S.M. Oh, J. Electrochem. Soc. 154 (2007) A1112.
[18] X.L. Yang, P.C. Zhang, Z.Y. Wen, L.L. Zhang, J. Alloys Compd. 496 (2010) 403–406.
[19] W. Xing, A.M. Wilson, K. Eguchi, G. Zank, J.R. Dahn, J. Electrochem. Soc. 144 (1997) 2410.
[20] D. Ahn, R. Raj, J. Power Sources 196 (2011) 2179–2186.
[21] B. Gao, S. Sinha, L. Fleming, O. Zhou, Adv. Mater. 13 (2001) 816.
[22] B.K. Guo, J. Shu, Z.X. Wang, H. Yang, L.H. Shi, Y. Liu, L.Q. Chen, Electrochem. Commun. 10 (2008) 1876–1878.
[23] Z.P. Guo, D.Z. Jia, L. Yuan, H.K. Liu, J. Power Sources 159 (2006) 332–335.